Adaptive Backstepping Active Fault-Tolerant Control with Nonlinear Adaptive Observer for Quadrotor UAV Under Actuator Faults and Disturbances

Abderrahim EZZARA[1]*, Ahmed Youssef OUADINE[2], Hassan AYAD[1]

[1] LSEEET Laboratory, Department of Applied Physics, Faculty of Science and Technology, Cadi Ayyad University, Gueliz, Marrakesh, 40000, Morocco
ezzara.abderrahim@gmail.com (**Corresponding author*), h.ayad@uca.ma

[2] Ecole Royale de l'Air, Marrakesh, 40000, Morocco
a.y.ouadine@gmail.com

Abstract: This paper presents a robust active fault-tolerant control (AFTC) strategy for quadrotor unmanned aerial vehicles (UAVs) that addresses actuator faults and external disturbances within a nonlinear system. Thus, this approach involves using a comprehensive nonlinear model of a quadrotor. In order to enable the simultaneous estimation of the system states and actuator faults, a nonlinear adaptive observer (AO) was designed. This observer does not require the conventional observer matching condition and it employs a LMI-based optimisation approach, which simplifies the design process. Building on this, an adaptive backstepping FTC (ABFTC) technique is proposed, which utilises an AO-based fault estimation (FE) to compensate for the actuator faults and an adaptive control law for estimating the external disturbances. Furthermore, an adaptive algorithm is integrated into the FE unit to decouple the disturbances from the actuator fault estimates. The stability of this closed-loop system is validated through the Lyapunov theory and the effectiveness of the proposed FTC strategy is validated through MATLAB simulations.

Keywords: Active fault-tolerant control, Quadrotor unmanned aerial vehicles, Nonlinear adaptive observer, Actuator faults, External disturbances, Adaptive backstepping.

1. Introduction

In the last few years, quadrotors, as unmanned aerial vehicles (UAVs), have garnered significant attention and they were widely adopted across various sectors, including commercial, industrial, and military applications. However, despite their many advantages, quadrotors are vulnerable to actuator faults and external disturbances, which can critically affect their stability. To address these challenges, actuator fault-tolerant control (FTC) systems have become a focal point of research.

FTC systems can either have a passive design, which treats faults as perturbations and uses general optimisation methods, which can be limiting or an active design, which utilises a detailed fault estimation (FE) using observer-based methods (Lan & Patton, 2016) and a recovery module that takes the necessary actions to correct the faulty system for precise control adjustments and adaptability (Jain, J. Yamé, & Sauter, 2018). Among the most commonly used techniques for the recovery module of FTC systems are sliding mode control (SMC) and backstepping.

Backstepping has become an attractive control technique for dealing with issues associated with underactuated systems, such as quadrotors.

Many control techniques based on backstepping have been proposed without considering the impacts of faults or disturbances, for example in (Bouadi, Bouchoucha & Tadjine, 2007) and (Saibi, Boushaki & Belaidi, 2022).

There have been several ideas for addressing the impacts of disturbances in the context of backstepping control systems, such as in (Huo, Huo & Karimi, 2014; Xuan-Mung & Hong, 2019; Karahan, Kasnakoglu & Nuri Akay, 2023). However, these papers do not address the faults within the system.

In (Khebbache et al., 2012; Mlayeh & Ben Othman, 2022; Mlayeh & Khedher, 2024), the authors propose a passive FTC technique based on a backstepping approach to overcome the effect of actuator faults without considering the effect of disturbances.

The existing control techniques based on backstepping have made significant strides, but many either do not account for both disturbances and faults or focus on one aspect while neglecting the other. To that, the proposed backstepping-based FTC techniques are mostly passive strategies.

Despite its advantages, traditional backstepping, unlike conventional SMC, is sensitive to disturbances. However, practically, the upper bound of external disturbances, which is necessary for the traditional SMC, is challenging to determine perfectly a priori. These limitations highlight the

https://doi.org/10.24846/v34i1y202507

necessity of improving backstepping by integrating it with other techniques, such as adaptive control, fuzzy logic, or neural networks. Such enhancements can help mitigate the impact of disturbances and improve the controller's robustness.

In this study, these gaps are addressed by proposing a novel backstepping-based active FTC strategy that simultaneously tackles both external disturbances and actuator faults.

In the field of active FTC, there is now an extensive amount of research on FE techniques, principally based on adaptive observers (AOs) and sliding-mode observers (SMOs) (Lan & Patton, 2016). AOs enable us to estimate faults when they are modeled as changes in parameters.

For FE, several authors have used adaptive observers (Besançon, 2007; Zhang, Jiang & Cocquempot, 2008). However, they make the assumption that the number of measured outputs and the transfer functions between faults are strictly positive real (SPR), however, for many real-world systems, including quadrotors, this is not the case. A new adaptation law with relaxed SPR is proposed by Oucief, Tadjine, & Labiod (2016).

This paper is based on the joint use of an AO for FE, and an adaptive backstepping FTC (ABFTC) technique for stabilizing the faulty system and for disturbance estimation and compensation.

The primary contributions of this study are the following: (1) using a comprehensive nonlinear model of the quadrotor UAV that accounts for the system's nonlinearities and high-order nonholonomic constraints; (2) a nonlinear AO is used to estimate both system states and actuator faults simultaneously, without requiring the traditional observer matching condition. This approach effectively handles faults that affect unmeasured state dynamics. The observer design is simplified through a linear matrix inequality (LMI) optimisation approach; (3) using the AO-based FE, an ABFTC controller is proposed for compensating for external disturbances and actuator faults; (4) the ABFTC is meant to estimate the unknown external disturbances and compensate for their effect without the need for a precise upper bound for external disturbances; (5) an adaptive law is designed to decouple disturbances from actuator fault estimates in order to obtain a more accurate FE.

The remainder of this paper is organised as follows. Section 2 provides a short explanation of the system's nonlinear dynamic model. In Section 3, a nonlinear AO is introduced to estimate the faults and next a novel law is proposed for decoupling disturbances from actuator fault estimates. Section 4 presents a robust adaptive backstepping control technique that is used for handling external disturbances and failure effects. Further on, Section 5 presents the validation of the FTC strategy using MATLAB simulations. Finally, Section 6 sets forth the conclusion of this paper.

2. Quadrotor Modeling

Let's consider an inertial frame E (O, X, Y, Z), and let B (o, x, y, z) designate a frame that is permanently coupled to the quadrotor, as illustrated in Figure 1. The quadrotor's absolute position is defined by the three coordinates (x, y, z) and its attitude by the three Euler's angles (φ, θ, ψ), namely roll, pitch, and yaw.

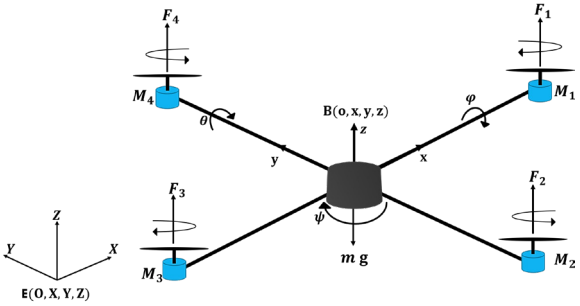

Figure 1. The quadrotor configuration

The quadrotor model is provided as in (Bouadi, Bouchoucha & Tadjine, 2007) by:

$$\ddot{\varphi} = \frac{1}{I_x}\left(\dot{\theta}\dot{\psi}(I_y - I_z) - K_{fax}\dot{\varphi}^2 - J_r\bar{\Omega}\dot{\theta} + dU_2\right) \tag{1a}$$

$$\ddot{\theta} = \frac{1}{I_y}\left(\dot{\varphi}\dot{\psi}(I_z - I_x) - K_{fay}\dot{\theta}^2 + J_r\bar{\Omega}\dot{\varphi} + dU_3\right) \tag{1b}$$

$$\ddot{\psi} = \frac{1}{I_z}\left(\dot{\theta}\dot{\varphi}(I_x - I_y) - K_{faz}\dot{\psi}^2 + U_4\right) \tag{1c}$$

$$\ddot{x} = \frac{1}{m}\left((C\varphi S\theta C\psi + S\varphi S\psi)U_1 - K_{ftx}\dot{x}\right) \tag{1d}$$

$$\ddot{y} = \frac{1}{m}\left((C\varphi S\theta S\psi - S\varphi C\psi)U_1 - K_{fty}\dot{y}\right) \tag{1e}$$

$$\ddot{z} = \frac{1}{m}\left(C\varphi C\theta U_1 - K_{ftz}\dot{z}\right) - \mathrm{g} \tag{1f}$$

where:

- C is the cosine function, and S is the sine function;
- I_x, I_y and I_z are the constant's inertia;

- K_{fax}, K_{fqy} and K_{faz} are the aerodynamic friction coefficients around X, Y, and Z;
- J_r is the rotor inertia;
- $\bar{\Omega}$ is the disturbance due to the rotor imbalance;
- d is the distance between the quadrotor centre of gravity and the rotation axis of propellers;
- m is the quadrotor's mass;
- g is the gravity acceleration constant;
- K_{ftx}, K_{fty} and K_{ftz} represent the translation drag coefficients;
- U_1, U_2, U_3, and U_4 represent the control inputs of the system.

U_1, U_2, U_3, and U_4 are expressed based on the angular speeds ω_i (for $i \in \{1, 2, 3, 4\}$) of the four propellers as follows:

$$\begin{bmatrix} U_1 \\ U_2 \\ U_3 \\ U_4 \end{bmatrix} = \begin{bmatrix} K_p & K_p & K_p & K_p \\ -K_p & 0 & K_p & 0 \\ 0 & -K_p & 0 & K_p \\ K_d & -K_d & K_d & -K_d \end{bmatrix} \begin{bmatrix} \omega_1^2 \\ \omega_2^2 \\ \omega_3^2 \\ \omega_4^2 \end{bmatrix} \tag{2}$$

$$\bar{\Omega} = \omega_1 - \omega_2 + \omega_3 - \omega_4 \tag{3}$$

The control inputs remain restricted by the motors' maximum rotational speeds ω_{max}, which are illustrative of their physical constraints:

$$\begin{aligned} &0 \le U_1 \le 4K_p\,\omega_{\max}^2 \\ &-K_p\,\omega_{\max}^2 \le U_2 \le K_p\,\omega_{\max}^2 \\ &-K_p\,\omega_{\max}^2 \le U_3 \le K_p\,\omega_{\max}^2 \\ &-2K_d\,\omega_{\max}^2 \le U_4 \le 2K_d\,\omega_{\max}^2 \end{aligned} \tag{4}$$

The high-order nonholonomic constraints may be obtained from the translation dynamics equations (1a)-(1f):

$$\sin\varphi = \frac{\left(\ddot{x} + \frac{K_{ftx}}{m}\dot{x}\right)S\psi - \left(\ddot{y} + \frac{K_{fty}}{m}\dot{y}\right)C\psi}{\sqrt{\left(\ddot{x} + \frac{K_{ftx}}{m}\dot{x}\right)^2 + \left(\ddot{y} + \frac{K_{fty}}{m}\dot{y}\right)^2 + \left(\ddot{z} + g + \frac{K_{ftz}}{m}\dot{z}\right)^2}} \tag{5a}$$

$$tan\theta = \frac{\left(\ddot{x} + \frac{K_{ftx}}{m}\dot{x}\right)C\psi + \left(\ddot{y} + \frac{K_{fty}}{m}\dot{y}\right)S\psi}{\ddot{z} + g + \frac{K_{ftz}}{m}\dot{z}} \tag{5b}$$

This corrective block will be used to generate the intended roll (φ_d) and pitch (θ_d).

3. The Adaptive Observer

3.1 Adaptive Observer Design

The system state space in equations (1a)-(1f), including actuator faults, is given by:

$$\begin{cases} \dot{x}(t) = Ax(t) + B\Phi(x,u) + \eta(y,u) + Ef(x) \\ y(t) = Cx(t) \end{cases} \tag{6}$$

where $x \in \mathbb{R}^{12}$ is the state vector of the system, which can be expressed as:

$$x = \left[x_1, \ldots, x_{12}\right]^T = \left[\varphi, \theta, \psi, x, y, z, \dot{\varphi}, \dot{\theta}, \dot{\psi}, \dot{x}, \dot{y}, \dot{z}\right]^T \tag{7}$$

where x_i for $i \in \{1, 12\}$ denotes the system states. $A \in \mathbb{R}^{12\times12}$, $B \in \mathbb{R}^{12\times14}$, $E \in \mathbb{R}^{12\times4}$, and $C \in \mathbb{R}^{6\times12}$ are known constant matrices. $f(x) = \sigma(x)f_a(t)$, is the resultant of the actuator faults, where $f_a \in \mathbb{R}^4$ represent the actuator fault vector, with $f_a = [f_{a1}, f_{a2}, f_{a3}, f_{a4}]$. $\sigma(x) : \mathbb{R}^{12} \to \mathbb{R}^{4\times4}$ is a known function matrix that might have nonlinear dependencies on x and $\eta(y, u)$ and $\Phi(x, u)$ are known nonlinear function vectors. $u = [U_1, U_2, U_3, U_4]^T$ is the input control vector, and $y \in \mathbb{R}^6$ is the system output expressed as $y = [\varphi, \theta, \psi, x, y, z]^T$.

In this paper, the system model in equation (6) satisfies the following conditions:

C0: The pair (C, A) is observable;

C1: $\eta(y, u)$ is continuous in y and u;

C2: $\sigma(x)$ and $\Phi(x, u)$ fulfill the Lipschitz property, i.e. there exist positive constants γ_1 and γ_2 such that for all x, $\hat{x} \in \mathbb{R}^{12}$:

$$\| \Phi(x,u) - \Phi(\hat{x},u) \| \le \gamma_1 \| x - \hat{x} \| \tag{8a}$$

$$\| \sigma(x) - \sigma(\hat{x}) \| \le \gamma_2 \| x - \hat{x} \| \tag{8b}$$

C3: The actuator fault vector f_a is bounded and piecewise constant:

$$\left\| f_a(t) \right\| \le \gamma_3 \tag{9}$$

where γ_3 is a known positive constant.

C4: The matrix $E\,\sigma(x)$ is persistently exciting, such that for all $t \ge 0$:

$$n_1 I_{12} \ge \int_t^{t+\tau} E\ \sigma(x)\sigma(x)^T E^T dt \ge n_2 I_{12} \tag{10}$$

where τ, n_1 and n_2 are positive constants. $I_{12} \in \mathbb{R}^{12\times12}$ represents the identity matrix.

The standard form of the AO for the system in equation (6) is given in (Cho & Rajamani, 1997).

To be used in FE, the system must be satisfying the famous matching condition given by:

$$E^T P = FC \tag{11}$$

The equality $E^T P = FC$ holds if and only if (Corless & Tu, 1998):

$$rank(CE) = rank(E) \tag{12}$$

In the case of the proposed model given in equations 1(a)-1(f) and (6), $rank(CE) = 0$ and $rank(E) = 4$. Unfortunately, the observer matching requirement in equation (12) is not fulfilled for this system, and therefore the standard form of the AO cannot be used.

In (Oucief, Tadjine & Labiod, 2016), the authors proposed a novel approach for developing an AO for a particular class of nonlinear systems.

For developing the considered adaptive observer, in addition to conditions C0, C1, C2 and C3 the system model in equation (6) has to fulfill the following conditions:

C5: The matrices A, B, C and E must satisfy the following:

$$CB = 0_{6\times 14} \tag{13a}$$
$$CE = 0_{6\times 4} \tag{13b}$$
$$rank(CAE) = rank(E) \tag{13c}$$

C6: Given bounded x, the first derivative in time of $\sigma(x)$ is continuous and bounded.

The system state space $x = [x_1,...,x_{12}]^{\mathrm{T}}$, as given in equation (7), is rearranged to satisfy condition C5 as follows:

$$\begin{aligned}
\dot{x}_1 &= x_7 \\
\dot{x}_2 &= x_8 \\
\dot{x}_3 &= x_9 \\
\dot{x}_4 &= x_{10} \\
\dot{x}_5 &= x_{11} \\
\dot{x}_6 &= x_{12} \\
\dot{x}_7 &= a_1 x_8 x_9 + a_2 x_7^2 + a_3 \bar{\Omega} x_8 + b_1 (U_2 + f_{a1}) \\
\dot{x}_8 &= a_4 x_7 x_9 + a_5 x_8^2 + a_6 \bar{\Omega} x_7 + b_2 (U_3 + f_{a2}) \\
\dot{x}_9 &= a_7 x_7 x_8 + a_8 x_9^2 + b_3 (U_4 + f_{a3}) \\
\dot{x}_{10} &= a_9 x_{10} + U_x \frac{U_1}{m} \\
\dot{x}_{11} &= a_{10} x_{11} + U_y \frac{U_1}{m} \\
\dot{x}_{12} &= a_{11} x_{12} - \mathrm{g} + \frac{\cos(x_1)\cos(x_2)}{m}(U_1 + f_{a4})
\end{aligned} \tag{14}$$

where:

$$\begin{aligned}
a_1 &= \frac{I_y - I_z}{I_x} & a_2 &= \frac{-K_{fax}}{I_x} & a_3 &= \frac{-J_r}{I_x} \\
a_4 &= \frac{I_z - I_x}{I_y} & a_5 &= \frac{-K_{fay}}{I_y} & a_6 &= \frac{J_r}{I_y} \\
a_7 &= \frac{I_x - I_y}{I_z} & a_8 &= \frac{-K_{faz}}{I_z} & a_9 &= \frac{-K_{ftx}}{m} \\
a_{10} &= \frac{-K_{fty}}{m} & a_{11} &= \frac{-K_{ftz}}{m} & b_1 &= \frac{d}{I_x} \\
b_2 &= \frac{d}{I_y} & b_3 &= \frac{1}{I_z}
\end{aligned} \tag{15}$$

When these conditions are satisfied, a stable observer for the system in equation (6) has the form (Oucief, Tadjine, & Labiod , 2016)

$$\dot{\hat{x}} = A\hat{x} + B\Phi(\hat{x},u) + \eta(y,u) + E\hat{f}(\hat{x}) + L\,(y - C\hat{x}) \tag{16a}$$

$$\hat{f}_a = W + \Gamma\sigma^T(\hat{x})Hy \tag{16b}$$

$$\dot{W} = -\Gamma\frac{\mathrm{d}\sigma^T(\hat{x})}{\mathrm{d}t}Hy - \Gamma\sigma^T(\hat{x})\begin{bmatrix} HC\left(A\hat{x} + \eta(y,u)\right) + \\ G\left(y - C\hat{x}\right) \end{bmatrix} \tag{16c}$$

where $\hat{f}(\hat{x}) = \sigma(\hat{x})\hat{f}_a(t)$, and $\hat{f}_a$ is the actuator FE vector. $\Gamma = \Gamma^T > 0$ is the learning rate matrix, while H and G are constant matrices that need to be found.

Theorem 1. Under conditions C1, C2, C3, C5, and C6 the state estimate $\hat{x}$ converges to the real state x asymptotically, and $E\hat{f}(\hat{x})$ converges to $Ef(x)$ if there are positive real constants ε_1 and ε_2, and matrices $P = P^T > 0 \in \mathbb{R}^{12\times 12}$, $G \in \mathbb{R}^{4\times 6}$, and $H \in \mathbb{R}^{4\times 6}$ such that:

$$\begin{aligned}
\left(A - LC\right)^T P + P\left(A - LC\right) + \varepsilon_1 PBB^T P + \varepsilon_2 PEE^T P \\
+ \varepsilon_1^{-1}\gamma_1^2 I_{12} + \varepsilon_2^{-1}\gamma_2^2\gamma_3^2 I_{12} < 0
\end{aligned} \tag{17a}$$

$$HCA - GC = E^T P \tag{17b}$$

Furthermore, if $E\,\sigma(x)$ fulfills the persistent excitation (PE) condition given by C4, then $\hat{f}_a$ converges to f_a.

Conditions C0 to C6 are met for the proposed system, hence the adaption law in equation (16) is possible. To find the observer gains, (17a) and (17b) can be turned into a LMI optimisation problem. By applying the Schur complement (Boyd et al., 1994) and by considering $L = P^{-1}M$ for the inequality (17a), the following LMI is obtained:

$$\begin{bmatrix} \Lambda & PB & PE \\ B^T P & -\varepsilon_1^{-1} I_{14} & 0_{14\times 4} \\ E^T P & 0_{4\times 14} & -\varepsilon_2^{-1} I_4 \end{bmatrix} < 0 \tag{18}$$

with $\Lambda = A^T P + PA - C^T M^T - MC + \varepsilon_1^{-1}\gamma_1^2 I_{12} + \varepsilon_2^{-1}\gamma_2^2\gamma_3^2 I_{12}$.

Also, by applying the same technique utilised in (Corless & Tu, 1998), (17b) may be solved using:

$$\textit{Minimize } \delta \textit{ subject to}: \quad \begin{bmatrix} \delta I_4 & \Pi \\ \Pi^T & \delta I_{12} \end{bmatrix} \geq 0 \tag{19}$$

where $\Pi = HCA - GC - E^T P$, and δ is a positive scalar.

3.2 Disturbance Decoupling

It is supposed that the system attitude of the quadrotor is subject to external disturbances $d = [d_\varphi, d_\theta, d_\psi]^T$. The states x_7, x_8, and x_9 in equation (14) become:

$$\dot{x}_7 = a_1 x_8 x_9 + a_2 x_7^2 + a_3 \bar{\Omega} x_8 + b_1 \left(U_2 + f_{a1}\right) + \frac{1}{I_x} d_\varphi \tag{20a}$$

$$\dot{x}_8 = a_4 x_7 x_9 + a_5 x_8^2 + a_6 \bar{\Omega} x_7 + b_2 (U_3 + f_{a2}) + \frac{1}{I_y} d_\theta \tag{20b}$$

$$\dot{x}_9 = a_7 x_7 x_8 + a_8 x_9^2 + b_3 (U_4 + f_{a3}) + \frac{1}{I_z} d_\psi \tag{20c}$$

As a result, disturbances will significantly impair the accuracy of FE, resulting in an inaccurate FE and potential false alarms. To tackle this issue, an adaptive law is created to separate disturbances from actuator fault estimates:

$$\hat{f}_a^\dagger(t) = \hat{f}_a(t) - D\hat{d}(t) \tag{21}$$

where $\hat{f}_a^\dagger$ represents the improved fault estimate, $\hat{f}_a$ is the original fault estimate given by equation (16), $\hat{d} = [\hat{d}_\varphi, \hat{d}_\theta, \hat{d}_\psi]$ is the disturbance estimation vector, and $D = diag\,(\lambda_1, \lambda_2, \lambda_3)$ is a diagonal matrix with $\lambda_i \geq 0$ for $i \in \{1,2,3\}$. The parameters λ_i are determined through a tuning process based on simulation to optimise the disturbance decoupling and enhance the accuracy of FE.

Based on equation (21), the actuator fault estimate with an improved attitude becomes:

$$\begin{aligned} \hat{f}_{a1}^\dagger &= \hat{f}_{a1} - \lambda_1 \hat{d}_\varphi \Theta_1 \\ \hat{f}_{a2}^\dagger &= \hat{f}_{a2} - \lambda_2 \hat{d}_\theta \Theta_2 \\ \hat{f}_{a3}^\dagger &= \hat{f}_{a3} - \lambda_3 \hat{d}_\psi \Theta_3 \end{aligned} \tag{22}$$

where Θ_i for $i \in \{1,2,3\}$ are activation parameters given by:

$$\Theta_i = \begin{cases} 0 & if \quad \left|\hat{f}_{ai}\right| \leq \Delta_i \\ 1 & if \quad \left|\hat{f}_{ai}\right| > \Delta_i \end{cases} \tag{23}$$

where Δ_i for $i \in \{1,2,3\}$ is the threshold parameter.

4. The FTC Strategy of the Quadrotor

The proposed control approach is based on two loops, the internal loop has four control laws (U_1, U_2, U_3, and U_4), and the external loop has two virtual control laws (U_x and U_y). The synoptic scheme (Figure 2) below illustrates this control strategy.

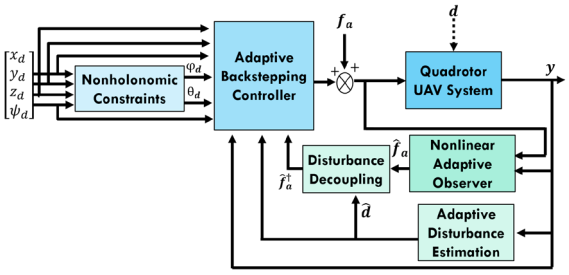

Figure 2. The proposed FTC structure

All phases of computation concerning Lyapunov functions and tracking errors are summarised as follows:

$$e_i = \begin{cases} x_i - x_{id} & i \in \{1,2,3,4,5,6\} \\ x_i - \dot{x}_{(i-6)d} + k_{(i-6)} e_{(i-6)} & i \in \{7,8,9,10,11,12\} \end{cases} \tag{24}$$

The related Lyapunov functions are provided by:

$$V_i = \begin{cases} \frac{1}{2} e_i^2 & i \in \{1,2,3,4,5,6\} \\ V_{i-6} + \frac{1}{2} e_i^2 & i \in \{7,8,9,10,11,12\} \end{cases} \tag{25}$$

The synthesised stabilising control laws are described in the following:

$$U_2 = \frac{1}{b_1}\left[\ddot{\varphi}_d - a_1 x_8 x_9 - a_2 x_7^2 - a_3 \bar{\Omega} x_8 - k_1(-k_1 e_1 + e_7) - e_1 - k_7 e_7 - \frac{1}{I_x}\hat{d}_\varphi\right] - \hat{f}_{a1}^\dagger - k_{a1} sign(e_7) \tag{26a}$$

$$U_3 = \frac{1}{b_2}\left[\ddot{\theta}_d - a_4 x_7 x_9 - a_5 x_8^2 - a_6 \bar{\Omega} x_7 - k_2(-k_2 e_2 + e_8) - e_2 - k_8 e_8 - \frac{1}{I_y}\hat{d}_\theta\right] - \hat{f}_{a2}^\dagger - k_{a2} sign(e_8) \tag{26b}$$

$$U_4 = \frac{1}{b_3}\left[\ddot{\psi}_d - a_7 x_7 x_8 - a_8 x_9^2 - k_3\left(-k_3 e_3 + e_9\right) - e_3 - k_9 e_9 - \frac{1}{I_z}\hat{d}_\psi\right] - \hat{f}_{a3}^\dagger - k_{a3} sign(e_9) \tag{26c}$$

$$U_x = \frac{m}{U_1}\left[\ddot{x}_d - a_9 x_{10} - k_4\left(-k_4 e_4 + e_{10}\right) - e_4 - k_{10} e_{10}\right] \tag{26d}$$

$$U_y = \frac{m}{U_1}\left[\ddot{y}_d - a_{10} x_{11} - k_5(-k_5 e_5 + e_{11}) - e_5 - k_{11} e_{11}\right] \tag{26e}$$

$$U_1 = \frac{m}{c x_1 c x_2}\left[\ddot{z}_d - a_{11} x_{12} + g - k_6\left(-k_6 e_6 + e_{12}\right) - e_6 - k_{12} e_{12}\right] - \hat{f}_{a4} - k_{a4} sign(e_{12}) \tag{26f}$$

where $k_i > 0$ for $i \in \{1,12\}$ and $k_{ai} > 0$ for $i \in \{1,2,3,4\}$.

Disturbance estimates are given by:

$$\dot{\hat{d}}_\varphi = \beta_1 e_7 \qquad \dot{\hat{d}}_\theta = \beta_2 e_8 \qquad \dot{\hat{d}}_\psi = \beta_3 e_9 \tag{27}$$

where $\beta_i > 0$ for $i \in \{1,2,3\}$.

Proof:

The expression of U_2 is demonstrated by considering the roll (φ) subsystem:

$$\begin{cases} \dot{x}_1 = x_7 \\ \dot{x}_7 = \Phi_1(x) + b_1 U_2(t) + b_1 f_{a1}(t) + \dfrac{1}{I_x} d_\varphi(t) \end{cases} \tag{28}$$

where $\Phi_1(x) = a_1 x_4 x_6 + a_2 x_2^2 + a_3 \bar{\Omega} x_4 . f_{a1}$ and d_φ are the actuator fault and disturbances that cannot be measured, respectively. The calculation of the control law U_2 is done in two steps.

Step 1: The first tracking error e_1 is examined, and provided by:

$$e_1 = x_1 - x_{1d} \tag{29}$$

The first Lyapunov function candidate is expressed as:

$$V_1(e_1) = \frac{1}{2} e_1^2 \tag{30}$$

The time derivative of equation (30) is given by:

$$\dot{V}_1(e_1) = e_1 \dot{e}_1 = e_1 (x_7 - \dot{x}_{1d}) \tag{31}$$

According to Lyapunov's theory, the stability of e_1 can be achieved by incorporating a new virtual control $(x_7)_d$ which represents the desired value of x_7:

$$(x_7)_d = \alpha_1 = \dot{x}_{1d} - k_1 e_1 \qquad (k_1 > 0) \tag{32}$$

Equation (31) then becomes $\dot{V}_1(e_1) = -k_1 e_1^2 \le 0$.

Step 2: As x_7 is not a real command, the following tracking-error variable e_7 is defined in relation to x_7 and α_1:

$$e_7 = x_7 - \alpha_1 = x_7 - \dot{x}_{1d} + k_1 e_1 \tag{33}$$

The augmented Lyapunov function is given by:

$$V_7(e_1, e_7) = V_1 + \frac{1}{2} e_7^2 \tag{34}$$

The time derivative of V_7 is given by:

$$\dot{V}_7(e_1, e_7) = e_1 \dot{e}_1 + e_7 \dot{e}_7 \tag{35}$$

Using $\dot{e}_1 = -k_1 e_1 + e_7$, equation (35) becomes:

$$\dot{V}_7(e_1, e_7) = e_1(-k_1 e_1 + e_7) + e_7 \left[\dot{x}_7 - \ddot{x}_{1d} + k_1(-k_1 e_1 + e_7)\right] \tag{36}$$

Substituting $\dot{x}_7$ by its expression, equation (36) yields:

$$\dot{V}_7(e_1, e_7) = e_1(-k_1 e_1 + e_7) + e_7[(\Phi_1 + b_1 U_2 + b_1 f_{a1} + \frac{1}{I_x} d_\varphi - \ddot{x}_{1d} + k_1(-k_1 e_1 + e_7)] \tag{37}$$

The stability of (e_1, e_7) may be achieved by adding the real input control U_2. Based on the principle of certain equivalence, $\hat{f}_{a1}$ and d_φ are replaced by their estimates:

$$U_2 = \frac{1}{b_1}\begin{pmatrix} \ddot{\varphi}_d - \Phi_1 - k_1(-k_1 e_1 + e_7) \\ -e_1 - k_7 e_7 - b_1 \hat{f}_{a1}^{\dagger} - b_1 \Gamma_1 - \dfrac{1}{I_x} \hat{d}_\varphi \end{pmatrix} \tag{38}$$

Equation (37) becomes:

$$\dot{V}_7(e_1, e_7) = -k_1 e_1^2 - k_7 e_7^2 + e_7 (b_1 \tilde{f}_{a1} - b_1 \Gamma_1 + \frac{1}{I_x} \tilde{d}_\varphi) \tag{39}$$

where $\tilde{f}_{a1} = f_{a1} - \hat{f}_{a1}^{\dagger}$ and $\tilde{d}_\varphi = d_\varphi - \hat{d}_\varphi$ (assuming that $\dot{d}_\varphi \approx 0$). The presence of term error $\tilde{d}_\varphi$ in the expression of $\dot{V}_7$ does not allow the determination of its sign. The Lyapunov function in equation (34) is increased by a square term to $\tilde{d}_\varphi$:

$$V^{\dagger}{}_7(e_1, e_7) = V_7(e_1, e_7) + \frac{1}{2\beta_1 I_x} \tilde{d}_\varphi^{\,2} \qquad (\beta_1 > 0) \tag{40}$$

The time derivative of $V_7^{\dagger}$ is expressed as:

$$\dot{V}_7^{\dagger}(e_1, e_7) = \dot{V}_7(e_1, e_7) - \frac{1}{\beta_1 I_x} \tilde{d}_\varphi \dot{\tilde{d}}_\varphi = -k_1 e_1^2 - k_7 e_7^2 + b_1 e_7 \left(\tilde{f}_{a1} - \Gamma_1\right) + \frac{1}{I_x} \tilde{d}_\varphi \left(e_7 - \frac{1}{\beta_1} \dot{\hat{d}}_\varphi\right) \tag{41}$$

Selecting a proper adaptation law for the estimate $\hat{d}_\varphi$ will eliminate the term of uncertainty. By choosing:

$$\dot{\hat{d}}_\varphi = \beta_1 e_7 \tag{42}$$

equation (41) becomes:

$$\dot{V}_7^{\dagger}(e_1, e_7) = -k_1 e_1^2 - k_7 e_7^2 - b_1 e_7 \left(\Gamma_1 - \tilde{f}_{a1}\right) \tag{43}$$

The presence of term errors denoted by $\tilde{f}_{a1}$ in the expression of $\dot{V}_7^{\dagger}$ does not allow the determination of its sign. By choosing:

$$\Gamma_1 = k_{a1} sign(e_7) \qquad (k_{a1} > 0) \tag{44}$$

Equation (43) then becomes:

$$\dot{V}_7^{\dagger}(e_1, e_7) \le -k_1 e_1^2 - k_7 e_7^2 - b_1 |e_7| \left(k_{a1} - |\tilde{f}_{a1}|\right) \tag{45}$$

It is supposed that an unknown parameter $k_{a1} > 0$ exists, such that:

$$|\tilde{f}_{a1}| \le k_{a1} \tag{46}$$

Finally, equation (45) becomes:

$$\dot{V}_7^{\dagger}(e_1, e_7) \le -k_1 {e_1}^2 - k_7 {e_7}^2 \le 0 \tag{47}$$

Finally,

$$U_2 = \frac{1}{b_1}\begin{bmatrix} \ddot{\varphi}_d - a_1 x_8 x_9 - a_2 x_7^2 - a_3 \bar{\Omega} x_8 - k_1\left(-k_1 e_1 + e_7\right) - \\ e_1 - k_7 e_7 - b_1 \hat{f}_{a1}^{\dagger} - b_1 k_{a1} sign\left(e_7\right) - \frac{1}{I_x}\hat{d}_{\varphi} \end{bmatrix} \tag{48}$$

By following the same steps, U_3, U_4, U_x, U_y and U_1 can be extracted.

High-frequency switching of the control signal can cause chattering, which wears down actuators and degrades the system performance. For this reason, the sign function may be substituted with another smooth function. In this paper, the following function is chosen:

$$sign(e_i) = \frac{e_i}{e_i + \varepsilon} \qquad i \in \{7, 8, 9, 12\} \tag{49}$$

where ε is a given small positive constant.

5. Simulation Results and Analysis

To evaluate the performance of the proposed ABFTC, simulations were executed in MATLAB/Simulink with a fundamental sample time of 0.001s. The quadrotor prototype for this study is the Draganfly IV, manufactured by "Draganfly Innovations". Parameter identification is analysed in (Derafa, Madani, & Benallegue, 2006) and summarised below:

Table 1. Quadrotor model parameters

Parameter	Value
m	400 *g*
g	9.81 $m{\cdot}s^{-2}$
d	25.5 *cm*
J_r	2.8385×10^{-5} N·*m* / rad / s^2
K_p	2.9842×10^{-5} N / rad / *s*
K_d	3.232×10^{-7} N·*m* / rad / *s*
I_x, I_y, I_z	$(3.828, 3.828, 7.135) \times 10^{-3}$ N·*m* / *rad* / s^2
$K_{ftx}, K_{fty}, K_{ftz}$	$(3.2, 3.2, 4.8) \times 10^{-2}$ *N* / *m* / *s*
$K_{fax}, K_{fay}, K_{faz}$	$(5.567, 5.567, 6.354) \times 10^{-4}$ *N* / *rad* / *s*

5.1 Observer Design

In this subsection, the parameters and the matrices of the observer are determined.

The values $\gamma_1 = 35$, $\gamma_2 = 2.06$, and $\gamma_3 = 10.2$ were chosen. Let $\varepsilon_1 = 76$ and $\varepsilon_2 = 80$.

The observer matrices are given by:

$$\begin{aligned}
&P = 10^3 \times \begin{bmatrix} P_{11} & P_{12} \\ {P_{12}}^T & 0_{6\times 6} \end{bmatrix} \\
&P_{11} = diag\left(8.598, 8.598, 7.683, 5.823, 5.823, 6.715\right) \\
&P_{12} = -10^{-2} \times diag\left(1.11, 1.11, 1.11, 1.19, 1.19, 1.12\right) \\
&M = 10^4 \times \begin{bmatrix} M_1 & M_2 \end{bmatrix}^T \\
&M_1 = diag\left(2.881, 2.881, 2.336, 0.709, 0.709, 1.240\right) \\
&M_2 = diag\left(0.846, 0.846, 0.755, 0.572, 0.572, 0.661\right) \\
&H = \begin{bmatrix} H_1 & 0_{4\times 1} & H_2 \end{bmatrix} \\
&H_1 = diag\left(0.0286, 0.0286, 0.0342, 0\right) \\
&H_2 = \begin{bmatrix} 0 & 0 & 0 & 0.0475 \end{bmatrix}^T \\
&L = 10^5 \times \begin{bmatrix} L_1 & L_2 \end{bmatrix}^T \\
&L_1 = 10^{-3} \times diag\left(7.6, 7.6, 6.1, 1.6, 1.6, 3.9\right) \\
&L_2 = diag\left(5.916, 5.916, 4.181, 0.795, 0.795, 2.307\right) \\
&\Gamma = 9.10^3 \times I_4 \qquad \delta = 1.0001 \times 10^{-5}
\end{aligned} \tag{50}$$

5.2 Simulation Parameters

In addition, to carry out realistic simulations, an additive Gaussian noise is introduced during all simulations for both disturbances and injected faults.

To simulate the nonlinear dynamics of the employed quadrotor in a real-world environment, the control inputs are constrained according to equation (4), based on the assumption that the maximum rotor speed is 8000 rpm. The linear velocities ($\dot{x}$, $\dot{y}$, and $\dot{z}$) and angular velocities ($\dot{\phi}$, $\dot{\theta}$, and $\dot{\psi}$) are bounded by practical values.

The proposed paths for the conducted simulations are selected so as to follow a helicoidal trajectory:

$$\psi_d\left(t\right) = \begin{cases} \dfrac{\pi}{6} & 15 \le t < 55 \\ -\dfrac{\pi}{6} & 70 \le t < 110 \end{cases} \tag{51}$$

with $x_d(t) = 22\sin(0.6t)$, $y_d(t) = 22\cos(0.6t)$ and $z_d(t) = 0.5t$.

The simulations were carried out for two scenarios, a fault-free case and a faulty case. Two time-varying actuator faults f_{a1} and f_{a4} associated

with the roll φ and altitude z commands are introduced. In addition, an additive Gaussian noise $\mathcal{N}_{a1}\left(0.05, 0.01^2\right)$ is added to f_{a1} and $\mathcal{N}_{a4}\left(0.01, 0.02^2\right)$ is added to f_{a4} with a sample time of $0.02s$ in both cases.

In both scenarios, the system is assumed to be affected by attitude disturbances, given as:

$$d_\varphi = d_\theta = 1\sin\left(0.2t\right) + \mathcal{N}_{\varphi,\theta}\left(0.0005, 0.0005^2\right)$$

$$d_\psi = 0.2\sin\left(0.2t\right) + \mathcal{N}_\psi\left(0.0001, 0.00005^2\right)$$

Disturbance decoupling parameters are established as: $\lambda_1 = 3.95$, $\lambda_2 = 3.95$, and $\lambda_3 = 1.04$.

5.3 Simulation Results

Based on the proposed ABFTC, Figure 3 provides a comparative analysis of the system's attitude and position states under fault-free and actuator fault conditions. It reveals that, despite the introduction of faults, the system states consistently converge to the desired values, indicating the ABFTC's efficacy in fault handling.

As observed, the roll and pitch angles are maintained within a moderate range of ±5°, these values effectively facilitating the quadrotor's smooth movement.

Figure 4, which depicts the tracking errors related to the system's attitude and position demonstrates the system's performance in both fault-free and faulty scenarios.

Figure 5 illustrates the disturbance estimation performance of the adaptive control law, it can be seen that the estimated disturbances align closely with the real ones, facilitating an effective decoupling from the system dynamics.

In Figure 6, the first image illustrates the real actuator fault f_{a1} alongside its estimates with and without disturbance decoupling. It is evident

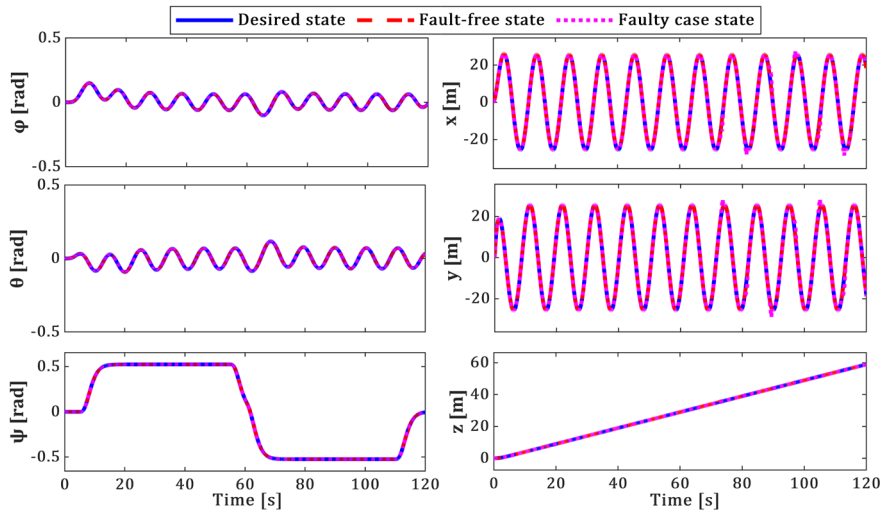

Figure 3. Attitude and position trajectories in the fault-free and faulty cases

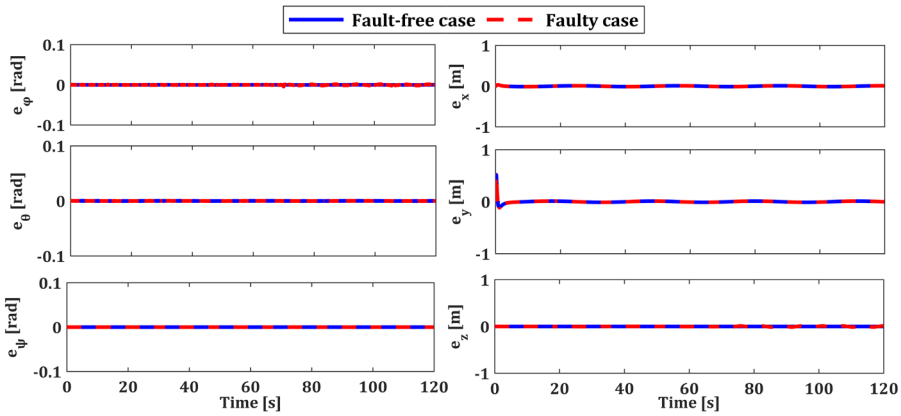

Figure 4. Tracking errors in the fault-free and faulty cases

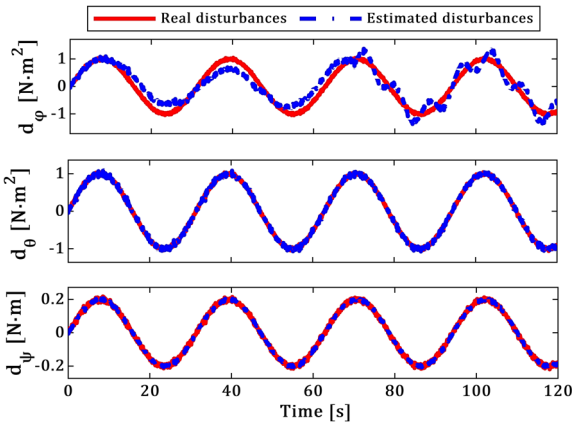

Figure 5. Attitude disturbance estimation

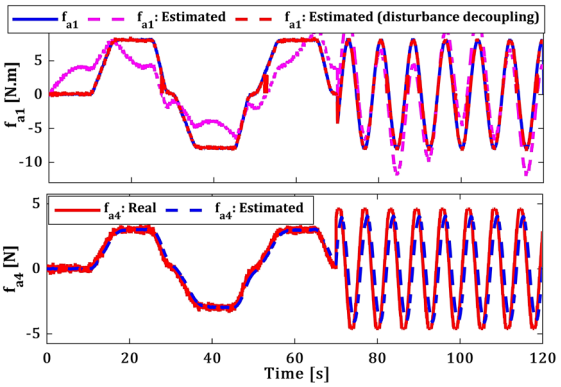

Figure 6. Actuator fault estimation performance

that the disturbance decoupling significantly enhances the accuracy of FE. The second image corroborates this by showing the estimation of f_{a4}, which closely matches the real fault.

Figure 7 displays the control inputs in the faulty case, revealing how the system adapts its control inputs to manage faults effectively. In spite of them, the quadrotor's closed-loop dynamics remains stable. Furthermore, this control approach provides input control signals that are both acceptable and physically achievable, reflecting the robustness and practicality of the proposed FTC approach. Also, it maintains a low energy consumption with small control inputs.

Figure 8 illustrates the quadrotor aircraft's 3D trajectory during its flight.

The simulation results show a good performance and resilience for trajectory tracking even after actuator faults occur.

To numerically evaluate the results obtained from the simulations, the RMSE (Root Mean Square Error) was calculated using certain established numerical criteria (Table 2).

Table 2. RMSE values for the attitude (in rad) and position (in m) trajectories

	Fault-free case	**Faulty case**
$RMSE_{\varphi}$	9.4×10^{-5}	3.4×10^{-4}
$RMSE_{\theta}$	9.4×10^{-5}	9.4×10^{-5}
$RMSE_{\psi}$	5.4×10^{-6}	5.4×10^{-6}
$RMSE_{x}$	2.2×10^{-2}	2.2×10^{-2}
$RMSE_{y}$	2.3×10^{-2}	2.3×10^{-2}
$RMSE_{z}$	7.7×10^{-6}	2.4×10^{-3}

While faults introduced in the roll (φ) and vertical (z) axis led to moderate increases in RMSE, the pitch (θ), yaw (ψ), and horizontal positions (x, y) remained unaffected, highlighting the controller's robustness. The relatively low increase in RMSE,

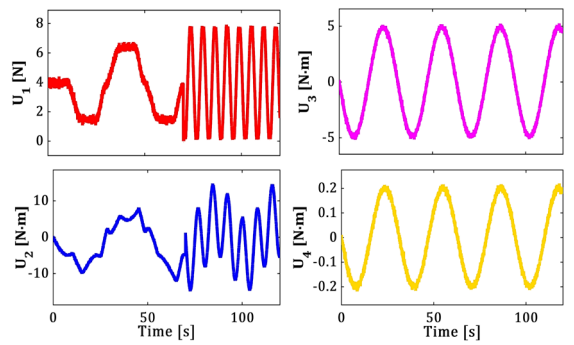

Figure 7. The control inputs of the actuators in the faulty case

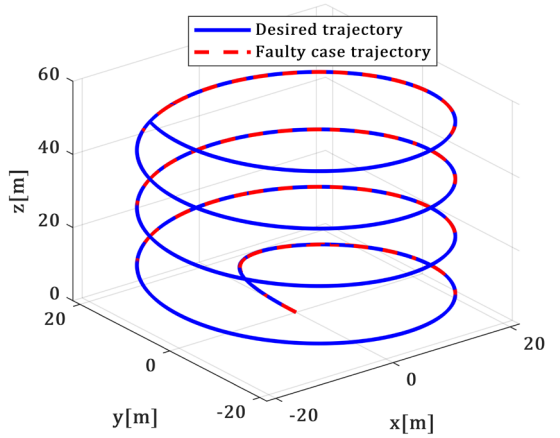

Figure 8. The quadrotor global trajectory in 3D in the faulty case

even in the faulty case, showcases the method's ability to isolate faults and maintain a stable system performance.

The RMSE values for the actuator fault estimation under various conditions are included in Table 3.

Table 3. RMSE values for the actuator FE under different conditions

	$\hat{f}_{a1}$	$\hat{f}_{a1}^{\dagger}$	$\hat{f}_{a4}$
Absence of f_{ai}	2.85	0.07	0.04
Absence of d_i	0.13	0.13	0.93
Presence of f_{ai} and d_i	2.85	0.36	0.93

As it can be seen in Table 3, in the fault-free case, where the system operates without faults but with disturbances, the disturbance decoupling significantly enhances the FE accuracy, with a RMSE of 0.07 *rad* for $\hat{f}_{a1}^{\dagger}$, in comparison with a RMSE of 2.85 *rad* for $\hat{f}_{a1}$ without decoupling. This improvement helps to accurately distinguish between faults and disturbances, thus preventing false alarms and avoiding incorrect fault declarations.

In the absence of disturbances, but where faults are present, the RMSE values for the improved and normal FE ($\hat{f}_{a1}^{\dagger}$ and $\hat{f}_{a1}$) are equal, indicating that the disturbance decoupling does not affect the FE accuracy when there are no disturbances. In the presence of faults and disturbances, the RMSE for $\hat{f}_{a1}^{\dagger}$ increases to 0.36 *rad* and the RMSE for $\hat{f}_{a1}$ is significantly higher at 2.85 *rad*, underscoring the critical importance of disturbance decoupling for maintaining an accurate FE.

Finally, for $\hat{f}_{a4}$, the RMSE is very low in the fault-free case (0.04 *rad*). However, in the faulty case scenario, the RMSE for $\hat{f}_{a4}$ increases to 0.93 *rad*.

6. Conclusion

This paper introduces a new active FTC strategy for diagnosing actuator faults in a quadcopter in the presence of external disturbances. Firstly, a complete dynamical model for a nonlinear quadrotor was introduced, taking into account several physical phenomena that might impact the proposed system's navigation in space. Secondly, to estimate the actuator faults, an AO has been developed, which does not require that the system meet the traditional observer matching condition. This approach effectively handles faults that affect the system`s unmeasured state dynamics. Thirdly, a new ABFTC controller was presented, in the presence of actuator faults and external disturbances, based on the adaptive backstepping technique. This controller utilizes the AO-based FE to compensate for actuator faults, and the external disturbances were estimated using an adaptive control law. In order to decouple disturbances from actuator fault estimates a novel adaptive FE law was proposed. Finally, several simulations were run in MATLAB to verify the effectiveness of the proposed strategy for a defective system. Two time-varying actuator faults related to the roll φ and the altitude z commands were introduced. In addition, disturbances and faults were coupled with additive Gaussian noises to simulate a realistic flight environment. The Root Mean Square Error (RMSE) was used to numerically assess the accuracy of the simulation results, providing a measure of the differences between the estimated and actual values.

The simulation results demonstrate the success of the proposed strategy. It allowed for a precise FE even in the presence of external disturbances and noise, as well as stability and trajectory tracking. Moreover, this control method provided physically achievable input control signals. The fact that the highest RMSE for system attitude in the faulty case is lower than 10^{-4} *rad*, and the highest RMSE for system position is lower than 10^{-2} *m* further highlights the proposed method's effectiveness in maintaining an accurate system control performance.

REFERENCES

Besançon, G. (2007) Parameter/Fault Estimation in Nonlinear Systems and Adaptive Observers. In: *Nonlinear Observers and Applications* (*Lecture Notes in Control and Information Sciences*, vol. 363). New York, USA, Springer, pp. 211-222.

Bouadi, H., Bouchoucha, M. & Tadjine, M. (2007) Modelling and Stabilizing Control Laws Design Based on Backstepping for A UAV Type-Quadrotor. *IFAC Proceedings Volumes*. 40(15), 245-250. https://doi.org/10.3182/20070903-3-FR-2921.00043.

Boyd, S., El Ghaoui, L., Feron, E. & Balakrishnan, V. (1994) *Linear Matrix Inequalities in System and Control Theory*. Philadelphia, Society for Industrial and Applied Mathematics.

Cho, Y.M. & Rajamani, R. (1997) A Systematic Approach to Adaptive Observer Synthesis for Nonlinear Systems. *IEEE Transactions on Automatic Control*. 42(4), 534-537. https://doi.org/10.1109/isic.1995.525102.

Corless, M. & Tu, J. (1998) State and Input Estimation for a Class of Uncertain Systems. *Automatica*. 34(6), 757-764. https://doi.org/10.1016/S0005-1098(98)00013-2.

Derafa, L., Madani, T., & Benallegue, A. (2006) Dynamic modelling and experimental identification of four rotors helicopter parameters. In: *2006 IEEE International Conference on Industrial Technology, 15-17 December 2006, Mumbai, India*. Piscataway, NJ, USA, IEEE. pp. 1834-1839.

Huo, X., Huo, M. & Karimi, H. (2014) Attitude Stabilization Control of a Quadrotor UAV by Using Backstepping Approach. *Mathematical Problems in Engineering*. 2014(10), Article ID 749803. https://doi.org/10.1155/2014/749803.

Jain, T., Yamé, J. J. & Sauter, D. (2018) *Active Fault-Tolerant Control Systems - A Behavioral System Theoretic Perspective*. Cham, Springer.

Karahan, M., Kasnakoglu, C. & Akay, A. N. (2023) Robust Backstepping Control of a Quadrotor UAV Under Pink Noise and Sinusoidal Disturbance. *Studies in Informatics and Control*. 32(2), 15-24. https://doi.org/10.24846/v32i2y202302.

Khebbache, H., Sait, B., Yacef, F. & Soukkou, Y. (2012) Robust Stabilization of A Quadrotor Aerial Vehicle in Presence of Actuator Faults. *International Journal of Information Technology, Control and Automation*. 2(2), 1-13. https://doi.org/10.5121/ijitca.2012.2201.

Lan, J. & Patton, R. (2016) Integrated fault estimation and fault-tolerant control for uncertain Lipschitz non-linear systems. *International Journal of Robust and Nonlinear Control*. 27(5), 761-780. https://doi.org/10.1002/rnc.3597.

Mlayeh, H. & Ben Othman, K. (2022) Nonlinear Accommodation of a DC-8 Aircraft Affected by a Complete Loss of a Control Surface. *Studies in Informatics and Control*. 31(3), 107-116. https://doi.org/10.24846/v31i3y202210.

Mlayeh, H. & Khedher, A. (2024) Actuator Fault Accommodation of an Aerial Vehicle Described by Takagi-Sugeno Models. *Studies in Informatics and Control*. 33(2), 73-81. https://doi.org/10.24846/v33i2y202407.

Oucief, N., Tadjine, M. & Labiod, S. (2016) A new methodology for an adaptive state observer design for a class of nonlinear systems with unknown parameters in unmeasured state dynamics. *Transactions of the Institute of Measurement and Control*. 40(4), 1297-1308. https://doi.org/10.1177/0142331216680288.

Saibi, A., Boushaki, R. & Belaidi, H. (2022) Backstepping Control of Drone. *Engineering Proceedings*. 14(1), 4. https://doi.org/10.3390/engproc2022014004.

Xuan-Mung, N. & Hong, S. K. (2019) Robust Backstepping Trajectory Tracking Control of a Quadrotor with Input Saturation via Extended State Observer. *Applied Sciences*. 9(23), 5184. https://doi.org/10.3390/app9235184.

Zhang, K., Jiang, B. & Cocquempot, V. (2008) Adaptive Observer-based Fast Fault Estimation. *International Journal of Control Automation and Systems*. 6(3), 320-326.